

La₂Co₂Se₂O₃: A Quasi-Two-Dimensional Mott Insulator with Unusual Cobalt Spin State and Possible Orbital Ordering

Cao Wang,[†] Ming-qiu Tan,[†] Chun-mu Feng,[‡] Zhi-feng Ma,[†] Shuai Jiang,[†] Zhu-an Xu,^{†,§} Guang-han Cao,^{*,†,§} Kazuyuki Matsubayashi,^{||} and Yoshiya Uwatoko^{||}

Department of Physics, Test and Analysis Center, and State Key Lab of Silicon Materials, Zhejiang University, Hangzhou 310027, People's Republic of China, and Institute for Solid State Physics, The University of Tokyo, Kashiwanoha, Kashiwa, Chiba 277-8581, Japan

Received January 7, 2010; E-mail: ghcao@zju.edu.cn

Abstract: The new oxyselenide La₂Co₂Se₂O₃, containing Co₂O square-planar layers, has been successfully synthesized using solid-state reactions under vacuum. The compound crystallizes in space group *I4/mmm* with lattice parameters $a = 4.0697(8)$ Å and $c = 18.419(4)$ Å. Magnetic susceptibility measurements indicate an antiferromagnetic transition at ~220 K. The magnetic entropy associated with the transition is close to $R \ln 2$, suggesting an unusual low-spin state for the Co²⁺ ions. The as-prepared sample shows insulating behavior with room-temperature resistivity of ~10⁷ Ω cm, which decreases by 4 orders of magnitude under a pressure of 7 GPa. Band structure calculations using the LSDA+*U* approach reproduce the insulating ground state with low spin for Co and suggest strong orbital polarization for the valence electrons near the Fermi level. It is also revealed that the spin and orbital degrees of freedom in the antiferromagnetic checkerboard spin–lattice are mutually coupled.

Introduction

The birth of high-temperature superconductivity¹ in layered copper oxides in the 1980s has stimulated intense explorations for new layered transition-metal compounds. In addition to a number of cuprate superconductors being discovered,^{2,3} more noncopper compounds have been synthesized and investigated. Remarkable examples include layered manganites with colossal magnetoresistance,⁴ layered cobaltates with a giant thermoelectric power^{5,6} and superconductivity,⁷ and newly discovered ferroarsenides with superconductivity up to 56 K.^{8,9}

The key structural units of cuprate and ferroarsenide superconductors are two-dimensional CuO₂ planes and Fe₂As₂ layers, respectively. Meanwhile, both of the parent compounds are associated with an antiferromagnetic (AFM) ground state. Therefore, transition-metal compounds with mixed anions

showing AFM order are appealing in search of novel superconducting materials. Fe₂La₂O₃E₂ (E = S, Se) is such a material, containing Fe₂O (so-called anti-CuO₂-type) layers and fluorite-type La₂O₂ layers.¹⁰ The compound and its analogues A₂F₂Fe₂OQ₂ (A = Sr, Ba; Q = S, Se)¹¹ indeed show AFM transitions around 100 K, representing a rare example of a frustrated AFM checkerboard spin–lattice.

In this paper we report the synthesis and characterization of the new cobalt oxyselenide La₂Co₂Se₂O₃ (the chemical formula here arranges the constituent elements in the order of electronegativity according to the general nomenclature of inorganic compounds). Powder X-ray diffraction (XRD) confirms that the compound is isostructural with Fe₂La₂O₃Se₂. The measurements of electrical resistivity, magnetic susceptibility, and specific heat indicate that it is an AFM Mott insulator with an unusual low-spin state for the Co²⁺ ions. Our first-principles calculations based on density functional theory not only reproduce the insulating ground state with low-spin configuration but also suggest orbital polarization for the valence electrons near the Fermi energy and mutual coupling between orbital and spin degrees of freedom in the AFM spin–lattice.

Experimental Section

La₂Co₂Se₂O₃ polycrystalline samples were synthesized by solid-state reactions under vacuum using powders of La₂O₃ and CoSe. La₂O₃ was dried by firing in air at 1173 K for 24 h prior to using. CoSe was presynthesized with the powders of Co and Se at 973 K for 24 h in an evacuated quartz ampule. All the starting materials were of high purity (≥99.95%). La₂O₃ and CoSe were weighed

[†] Department of Physics, Zhejiang University.

[‡] Test and Analysis Center, Zhejiang University.

[§] State Key Lab of Silicon Materials, Zhejiang University.

^{||} The University of Tokyo.

- (1) Bednorz, J. G.; Müller, K. A. *Z. Phys. B: Condens. Matter* **1986**, *64*, 189.
- (2) Cava, R. J. *J. Am. Ceram. Soc.* **2000**, *83*, 5.
- (3) Raveau, B.; Michel, C.; Hervieu, M.; Groult, D. In *Crystal Chemistry of High T_c Superconducting Copper Oxides*; Springer Verlag: Berlin, 1991.
- (4) Kimura, T.; Tokura, Y. *Annu. Rev. Mater. Sci.* **2000**, *30*, 451.
- (5) Terasaki, I.; Sasago, Y.; Uchinokura, K. *Phys. Rev. B* **1997**, *56*, 12685.
- (6) Masset, A. C.; Michel, C.; Maignan, A.; Hervieu, M.; Toulemonde, O.; Studer, F.; Raveau, B.; Hejtmanek, J. *Phys. Rev. B* **2000**, *62*, 166.
- (7) Takada, K.; Sakurai, H.; Takayama-Muromachi, E.; Dilanian, R. A.; Sasaki, T. *Nature* **2003**, *422*, 53.
- (8) Kamihara, Y.; Watanabe, T.; Hirano, M.; Hosono, H. *J. Am. Chem. Soc.* **2008**, *130*, 3296.
- (9) Wang, C.; Li, L. J.; Chi, S.; Zhu, Z. W.; Ren, Z.; Li, Y. K.; Wang, Y. T.; Lin, X.; Luo, Y. K.; Jiang, S.; Xu, X. F.; Cao, G. H.; Xu, Z. A. *Europhys. Lett.* **2008**, *83*, 67006.

(10) Mayer, J. M.; Schneemeyer, L. F.; Siegrist, T.; Waszczak, J. V.; Dover, B. V. *Angew. Chem., Int. Ed. Engl.* **1992**, *31*, 1645.

(11) Kabbour, H.; Janod, E.; Corraze, B.; Danot, M.; Lee, C.; Whangbo, M. H.; Cario, L. *J. Am. Chem. Soc.* **2008**, *130*, 8261.

according to the stoichiometric ratio, thoroughly mixed in an agate mortar, and pressed into pellets under a pressure of 8000 kg/cm². All these procedures were performed in a glovebox filled with high-purity argon. The pellets were sealed in evacuated quartz tubes and then heated uniformly at 1373 K for 40 h. The solid-state reaction was repeated once or twice with intermediate regrinding.

Powder XRD was performed at room temperature using a D/Max-rA diffractometer with Cu K α radiation and a graphite monochromator. The detailed structural parameters were obtained by Rietveld refinement,¹² using the step-scan data in the range of $10^\circ \leq 2\theta \leq 120^\circ$. The dc electrical resistivity was measured by employing a two-terminal method with the configuration like a parallel-plate capacitor to decrease the sample's resistance (over 1 M Ω). The room-temperature resistance under high pressure was measured using a cubic anvil. The electric current through the sample was below 1 μ A, and the internal resistance of the voltmeter was 1 G Ω . The measurement of dc magnetic susceptibility was conducted on a Quantum Design Magnetic Property Measurement System (MPMS-5). The applied field was 1000 Oe. The measurement of specific heat was carried out on a Quantum Design Physical Property Measurement System (PPMS-9), using a thermal relaxation method.

To obtain information about the spin and orbital states in La₂Co₂Se₂O₃, we applied first-principles calculations on the basis of density functional theory using the approach of local-spin density approximation plus on-site Coulomb interaction U (LSDA+ U).¹³ A full-potential minimum-basis local-orbital scheme (FPLO) is employed to solve the Kohn–Sham equations on a regular lattice.¹⁴ In this method relativistic effects can be treated in a related four-component code, and the LSDA+ U formalism is implemented. We considered a probable checkerboard AFM lattice for the cobalt spins,¹¹ where the space group should be changed into $P4_2/mmc$ (No. 131) from $I4/mmm$ (No. 139). The experimental lattice parameters were employed in our calculations. The k -mesh in the self-consistent calculation was set to $18 \times 18 \times 4$ (usually this is an accurate and safe setting). The on-site Coulomb interaction U and Hund's exchange parameter J were set to be 5 and 0.9 eV, respectively, which are reasonable and are widely used for 3d transition-metal oxides.

Results and Discussion

Figure 1 shows the structural characterization for the synthesized La₂Co₂Se₂O₃ sample by powder XRD experiment. Except for a few tiny peaks from La₂O₃, most of the XRD reflections can be indexed with a tetragonal unit cell. The diffraction index (hkl) obeys $h + k + l = \text{even numbers}$, suggesting a body-centered lattice. Thus, we adopted the structure model of Fe₂La₂O₃Se₂¹⁰ to perform a Rietveld refinement.¹² The refined cell parameters ($a = 4.0697(8)$ Å and $c = 18.419(4)$ Å) are reasonably smaller than those of Fe₂La₂O₃Se₂¹⁰ due to Co²⁺ ions being relatively smaller than Fe²⁺ ions. Detailed structural parameters are given in Table 1. In the crystal chemistry point of view, the structure (shown as an inset in Figure 1) can be described as an alternate stacking of fluorite-type [La₂O₂]²⁺ layers and antiperovskite-like [Co₂OSe₂]²⁻ layers (cf. [Sr₂CuO₂]²⁺ block layers in cuprate superconductors^{2,3}). The two block layers are connected by a CsCl-type structure.⁹ Using the well-defined empirical parameters in the literature,¹⁵ as well as the data of Co–Se and Co–O bond distances in Table 1, the bond valence sum (BVS) of the Co ions is calculated to be +1.98, very close to the apparent Co valence (+2) from the chemical formula.

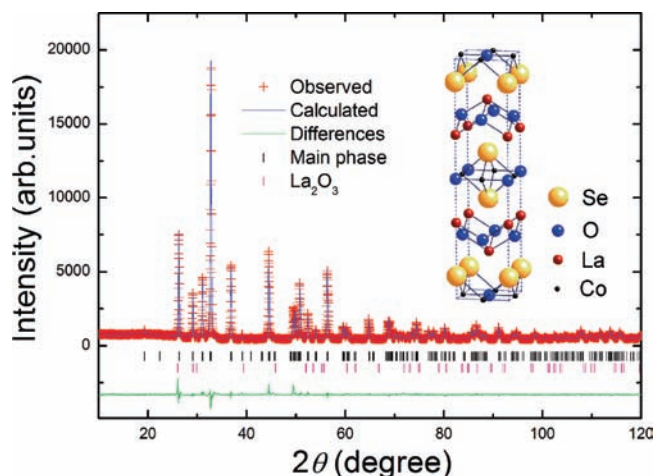


Figure 1. Rietveld refinement profile on the powder X-ray diffraction data for La₂Co₂Se₂O₃. The mass fraction of La₂O₃ impurity is 0.5%. The inset shows the crystal structure model employed.

Table 1. Room-Temperature Structural Parameters for La₂Co₂Se₂O₃ by the XRD Rietveld Refinement

chem formula	La ₂ Co ₂ Se ₂ O ₃			
space group	$I4/mmm$			
a (Å)	4.0697(8)			
c (Å)	18.419(4)			
V (Å ³)	305.06(10)			
R_{wp} (%)	5.23			
S	1.42			
Z	2			
density (g/cm ³)	6.549			
$d_{\text{Co-O}(2)}$ (Å)	2.035(1)			
$d_{\text{Co-Se}(4)}$ (Å)	2.688(1)			
atom	x	y	z	B_{50}
La	0.5	0.5	0.18370(5)	0.20(17)
Co	0.5	0	0	0.28(18)
Se	0	0	0.09533(7)	0.24(17)
O(1)	0.5	0	0.25	0.8(3)
O(2)	0.5	0.5	0	1.2(4)

Figure 2 shows resistivity measurement results for the as-prepared La₂Co₂Se₂O₃ sample. The room-temperature electrical resistivity measured is as high as $\sim 10^7$ Ω cm, three or four orders of magnitude higher than those of Fe₂La₂O₃Se₂¹⁰ and Ba₂F₂Fe₂OSe₂.¹¹ Furthermore, the temperature dependence of resistivity basically obeys thermally activated behavior: $\rho = \rho_0 \exp(E_a/k_B T)$, where ρ_0 refers to a prefactor and k_B is Boltzmann's constant. Using the $\rho(T)$ data from 260 to 320 K, the activation energy E_a was extracted to be 0.35 eV, which is substantially larger than that of Ba₂F₂Fe₂OSe₂.¹¹ The result suggests that the 3d electrons of Co²⁺, though being partially filled (3d⁷), are practically localized. The inset of Figure 2 shows the change in sample resistance under high pressures. It is striking that the resistance decreases by 4 orders of magnitude under a pressure of 7 GPa. The drastic pressure dependence of resistivity suggests the scenario of marginal Mott insulator where the Hubbard U is slightly larger than the bandwidth (see our band-structure calculation result below), because compressing the lattice generally leads to an increase in bandwidth, which suppresses the Mott gap, hence decreasing resistivity sharply.

The temperature dependence of magnetic susceptibility of La₂Co₂Se₂O₃ is presented in Figure 3. Above 300 K the susceptibility shows Curie–Weiss-like behavior, consistent with

(12) Izumi, F.; Ikeda, T. *Mater. Sci. Forum* **2000**, 321–324, 198.

(13) Anisimov, V. I.; Zaanen, J.; Andersen, O. K. *Phys. Rev. B* **1991**, 44, 943.

(14) Koepf, K.; Eschrig, H. *Phys. Rev. B* **1999**, 59, 1743.

(15) Brese, N. E.; O'Keeffe, M. *Acta Crystallogr.* **1991**, 47, 192.

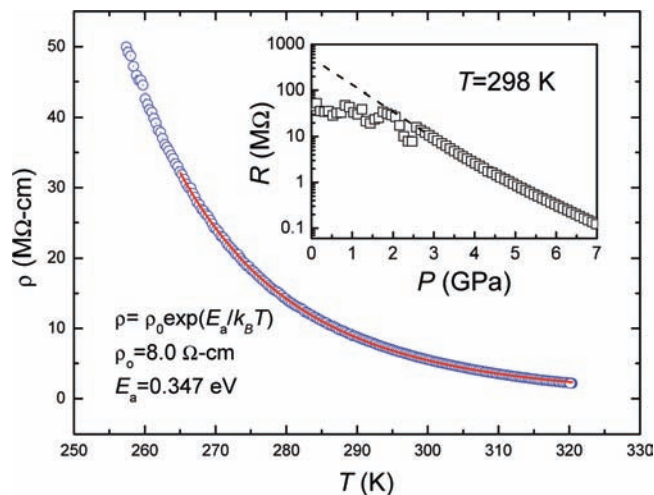


Figure 2. Temperature dependence of resistivity for the $\text{La}_2\text{Co}_2\text{Se}_2\text{O}_3$ polycrystalline sample. The inset shows the pressure dependence of resistance at room temperature. Note that the resistance at ambient pressure is too high to be measured accurately.

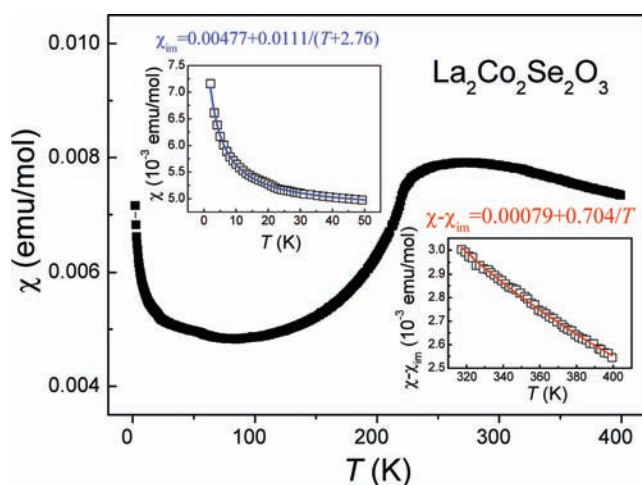


Figure 3. Temperature dependence of the magnetic susceptibility for $\text{La}_2\text{Co}_2\text{Se}_2\text{O}_3$. The applied field is 1000 Oe. The data fittings in the insets are based on Curie–Weiss law.

the picture of localized magnetism for the cobalt atoms. In the temperature range from ~ 220 to 300 K, there is a broad maximum, which is a signature of low-dimensional magnetism with AFM correlations. Around $T_N = 220$ K an abrupt decrease in susceptibility takes place, suggesting an AFM transition. A similar susceptibility anomaly due to AFM transition was observed at 80–100 K in $\text{Fe}_2\text{La}_2\text{O}_3\text{Se}_2$ ¹⁰ and $\text{Ba}_2\text{F}_2\text{Fe}_2\text{OSe}_2$.¹¹ The susceptibility upturn below 50 K, which can be fitted with an extended Curie–Weiss formula, $\chi(T) = \chi_0 + C_{\text{imp}}/(T - \Theta_p)$, is probably due to lattice imperfections and/or paramagnetic impurities such as CoSeO_3 (from the fitted C_{imp} value and the effective moment of free Co^{2+} ($4.8 \mu_B/\text{Co}$), the impurity molar fraction was estimated to be less than 0.4%, which might not be detected by XRD).

In the high-temperature ($T \gg T_N$) limit, $\chi(T)$ should obey Curie–Weiss law. Considering that ferromagnetic (FM) and AFM couplings within the Co_2O checkerboard spin–lattice may cancel each other to some extent (see below for further discussions), we fitted the $\chi(T)$ data in the range of $317 \text{ K} < T < 400 \text{ K}$ assuming $\Theta_p = 0$. The result gives the Curie constant $C = 0.352 \text{ emu K}/(\text{mol of Co})$, corresponding to the effective

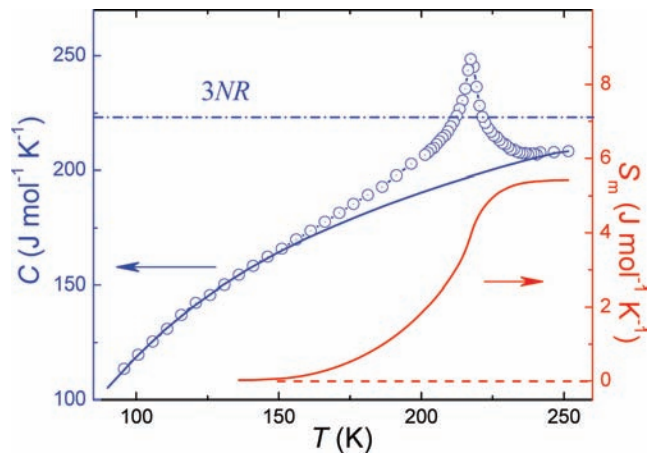


Figure 4. Temperature dependence of specific heat for $\text{La}_2\text{Co}_2\text{Se}_2\text{O}_3$. The solid curve represents the lattice contribution, fitted by a polynomial. The right label denotes the magnetic entropy associated with the antiferromagnetic transition.

magnetic moment $\mu_{\text{eff}} = 1.68 \mu_B/\text{Co}$. There are two alternative spin states for Co^{2+} ions: either low spin (LS) with $S = 1/2$ or high spin (HS) with $S = 3/2$. The result favors the LS configuration because the spin-only moments for the LS and HS states are 1.73 and $3.87 \mu_B/\text{Co}$, respectively.

In order to further understand the magnetic transition, we performed a specific heat measurement. As shown in Figure 4, the high-temperature specific heat approaches the value of $3NR$, where $N = 9$ and $R = 8.314 \text{ J mol}^{-1} \text{ K}^{-1}$ (N is the number of atoms in the chemical formula; R refers to the gas constant), in accordance with the Dulong–Petit law. Indeed, a heat-capacity peak appears at 220 K, consistent with the magnetic susceptibility data above. Note that it is a second-order phase transition, since the peak does not shift for cooling and heating processes. By neglect of the magnon contribution at very low temperatures ($T \ll T_N$), the specific heat can be separated into electronic and phonon parts: $C(T) = \gamma T + \beta T^3$. We found that the low-temperature data ($2 \text{ K} < T < 10 \text{ K}$) show almost no electronic contribution (the electronic specific-heat coefficient is less than $0.002 \text{ J mol}^{-1} \text{ K}^{-2}$), consistent with the insulating ground state. From the slope (β) of the straight line in the C/T vs T^2 plot (not shown here), we obtain the Debye temperature $\Theta_D = 234 \text{ K}$ using the formula $\Theta_D = [12\pi^4 NR/(5\beta)]^{1/3}$.

The entropy of the magnetic transition (S_{mag}) may also supply information on the spin state of Co^{2+} ions because S_{mag} should theoretically be close to $R \ln(2S + 1)$. Since the Debye model fails to reproduce the $C(T)$ data at high temperatures, we employ a polynomial to fit the phonon contribution (C_{ph}) in the temperature range from 95 to 255 K. Assuming that the total specific heat consists of phonon and magnetic components, the magnetic contribution (C_{mag}) can be obtained simply by the subtraction of C_{ph} . Consequently, the magnetic entropy can be calculated using the integral $S_{\text{mag}}(T) = \int_0^T C_{\text{mag}}/T \text{ d}T$. The result gives $S_{\text{mag}} = 5.43 \text{ J mol}^{-1} \text{ K}^{-1}$, which is 94% of $R \ln 2$ or 47% of $R \ln 4$, indicating that the Co^{2+} ions in $\text{La}_2\text{Co}_2\text{Se}_2\text{O}_3$ are truly in the LS state.

With respect to $3d^7$ configuration in an octahedral crystal field (CF), Co^{2+} usually exhibits an HS state. Due to the closeness of the CF splitting and Hund coupling energy, however, the exact spin state of cobalt may depend on the specific CF, Co

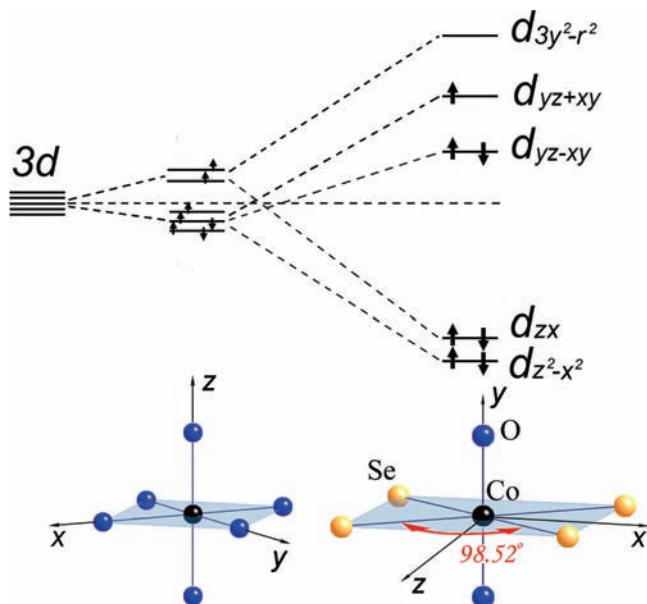


Figure 5. Crystal-field-splitting scheme and possible orbital occupations in the cases of regular and distorted octahedral coordination for Co^{2+} (d^7 configuration). Note that the Cartesian axes x , y , and z are parallel with the a , b , and c axes of the lattice, respectively. Therefore, for the $[\text{CoO}_2\text{Se}_4]$ coordination, the five commonly used Co 3d orbitals $3z^2 - r^2$, $x^2 - y^2$, xy , yz , and zx should be changed into $3y^2 - r^2$, zx , $z^2 - x^2$, $yz - xy$, and $yz + xy$ accordingly.

valence, and even temperature.^{5,16} When the CF splitting exceeds the Hund exchange, the LS state could be stabilized. In $\text{La}_2\text{Co}_2\text{Se}_2\text{O}_3$, the Co^{2+} ions are surrounded by two nearby oxygen anions and four distant selenium anions with bond lengths of $d_{\text{Co-O}} = 2.035(1)$ Å and $d_{\text{Co-Se}} = 2.688(1)$ Å. This highly distorted octahedral CF lifts the ordinary degeneracy of e_g and t_{2g} levels, as shown in Figure 5. Assuming point charges for the ligands, we calculated the CF splitting of the five 3d orbitals using standard CF theory¹⁷ for the real structure. The result shows that the distorted CF splitting between $d_{3y^2-r^2}$ and d_{yz-xy} levels (~ 40 meV) is much larger than the nondistorted splitting between e_g and t_{2g} levels (~ 7 meV), making the LS state probable for the Co^{2+} ions.

In addition to the above CF effect, the 3d-electron Coulomb interaction and the p-d hybridization also play important roles in determining the ground-state properties for most transition-metal oxides. We thus carried out band-structure calculations using the LSDA+ U approach. The main results are displayed in the Supporting Information as well as in Figure 6. Here we summarize three points as follows.

First, our LSDA+ U calculations reproduce an insulating ground state, as indicated by the energy dependence of total density of state (DOS). The energy gap is 1.5 eV. Note that the activation energy E_a extracted from the resistivity measurement on polycrystalline samples often underestimates the band gap. One expects a future optical study to accurately determine the magnitude of the band gap.

Second, the LS state for Co^{2+} is confirmed by the calculated total moment of $0.84 \mu_B/\text{Co}$. The partial DOS data indicate that the occupancy of Co 3d states is 75% (33% spin-up and 42% spin-down), consistent with the d^7 configuration for Co^{2+} ions.

(16) Vogt, T.; Woodward, P. M.; Karen, P.; Hunter, B. A.; Henning, P.; Moodenbaugh, A. R. *Phys. Rev. Lett.* **2000**, *84*, 2969.

(17) Hotta, T. *Rep. Prog. Phys.* **2006**, *69*, 2061.

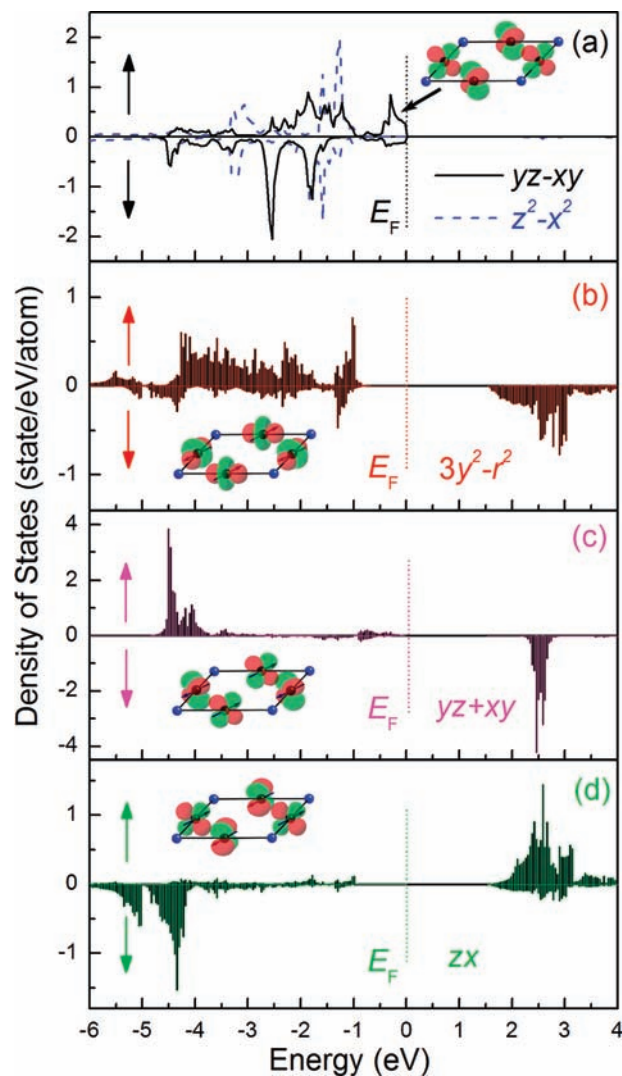


Figure 6. Orbital projected density of state for the cobalt atoms at $(\frac{1}{2}, 0, 0)$ in $\text{La}_2\text{Co}_2\text{Se}_2\text{O}_3$ from the LSDA+ U calculations. Fermi levels are set at zero energy. The up and down arrows represent the two different spin directions. The insets show the orbital polarization for the valence electrons near the Fermi level for (a) and possible spin/orbital orderings for (b)–(d).

The projected DOS for the Co atoms at $(\frac{1}{2}, 0, 0)$ shown in Figure 6 reveals that while the $z^2 - x^2$ and $yz - xy$ orbitals are fully filled, the other three orbitals are basically half-filled primarily because of the on-site Coulomb interaction. The orbital occupancy for $yz + xy$, $z^2 - x^2$, and $yz - xy$ is consistent with that expected from the CF analysis (Figure 5), but this is not true for the $3y^2 - r^2$ and zx cases. This inconsistency can be understood by the effect of p-d hybridization as well as Coulomb interaction. The $3y^2 - r^2$ and zx orbitals have their lobes directly toward the ligands, making stronger p-d hybridizations. The hybridization between Se 4p and Co 3d pushes the zx orbital higher in energy than $yz - xy$. As a result, the zx together with $3y^2 - r^2$ and $yz + xy$ orbitals becomes half filled because the Hubbard U is larger than the CF splitting. It is noted that the spin and orbital degrees of freedom are mutually coupled for $3y^2 - r^2$, zx , and $yz + xy$ orbitals. As shown in Figure 6b–d, the electron spin in the zx orbital is opposite to those in $3y^2 - r^2$ and $yz + xy$ orbitals.

Third, the valence-band electrons near the Fermi level (E_F) are orbitally polarized. These electrons have the orbital char-

acteristic of Co 3d, O₁ (within Co₂O planes) 2p, and Se 4p. In the energy range from -0.5 eV to E_F , the Co 3d electrons are dominated by the $yz - xy$ character (Figure 6a). Meanwhile, the O₁ 2p electrons are predominantly contributed by p_z . In contrast, no obvious orbital polarization is found for Se 4p (see Figure S1 in the Supporting Information).

For the Co atoms at $(0, \frac{1}{2}, 0)$, the notations of the 3d orbitals change by the transformation $x \rightarrow y$. Therefore, the above orbital occupancy represents a kind of orbital ordering, as shown in the insets of Figure 6. Remember that the 3d-orbital ordering was demonstrated not only in colossal magnetoresistance manganites¹⁸ but also in other transition-metal compounds.^{16,17,19} The present cobalt oxyselenide compound possibly exhibits another example of orbital ordering, which needs further experiments to confirm.

Now let us discuss the possible magnetic structure in La₂Co₂Se₂O₃. Reference 11 correctly considers three main magnetic exchange interactions in the checkerboard spin–lattice, namely one nearest-neighbor (J_1) and two next-nearest-neighbor (J_2 and J_2') exchange couplings. J_2 and J_2' denote the superexchanges via oxygen and selenium, respectively. As the active spins come from $3y^2 - r^2$, zx , and $yz + xy$ orbitals in [Co₂OSe₂]²⁻ layers, according to Goodenough–Kanamori rules,^{20,21} one expects a negative (AFM) J_2 due to 180° Co–O–Co superexchange and a positive (FM) J_2' due to ~90° Co–Se–Co superexchange. On the other hand, the direct exchange interaction J_1 is probably negative according to the result in ref 11. Therefore, this is also a magnetically frustrated system. The effective J_2 coupling will be weakened because of less spin polarization for $3y^2 - r^2$, as shown in Figure 6b, which could lead to the inequality $|J_2| < 2|J_1|$. In this circumstance,

according to the theoretical analysis in ref 11, the most stable spin structure simultaneously satisfies FM superexchange along [100] and [010] and AFM direct exchange along [110]. Further experiments such as neutron diffractions are called for to confirm the magnetic structure proposed.

Conclusion

To summarize, the new cobalt oxyselenide La₂Co₂Se₂O₃, containing anti-CuO₂-type Co₂O planes, was synthesized using solid-state reactions under vacuum. While being an analogue to Fe₂La₂O₃Se₂, it exhibits some different physical properties, including much higher room-temperature resistivity, greater activation energy, and higher AFM transition temperature. The most important difference is related to the spin state of the transition-metal ions. Our magnetic susceptibility and specific-heat measurements suggests an unusual LS state for Co²⁺ ions, which is reproduced by band-structure calculations. The LSDA+ U calculations also indicate orbital polarization for the valence electrons near the Fermi level, as well as the spin/orbital ordering due to mutual coupling between orbital and spin degrees of freedom. Considering the similarities in crystal/spin/orbital structure with the copper-based,^{1–3} iron-based,^{8,9} and cobalt-based superconductors,⁷ we claim that the present compound could be a parent material for exploring novel superconductivity and other quantum phenomena.

Acknowledgment. We acknowledge support from the NSF of China (Contract Nos. 90922002 and 10934005) and PCSIRT of the Ministry of Education of China (Contract No. IRT0754).

Supporting Information Available: CIF files giving X-ray crystallographic data and text and a figure giving supplementary band-structure calculation results. This material is available free of charge via the Internet at <http://pubs.acs.org>.

JA1001295

(18) Tokura, Y.; Nagaosa, N. *Science* **2000**, *288*, 462.

(19) Khomskii, D. I. *Phys. Scr.* **2005**, *72*, CC8.

(20) Goodenough, J. B. *Phys. Rev.* **1955**, *100*, 564.

(21) Kanamori, J. *Phys. Chem. Solids* **1959**, *10*, 87.